Eur. Phys. J. B **2**, 79–92 (1998)

THE EUROPEAN PHYSICAL JOURNAL B

Apparent slip at a polymer-polymer interface

J.L. Goveas[1,a] and G.H. Fredrickson[2]

[1] Materials Research Laboratory, University of California, Santa Barbara CA 93106-5130, USA
[2] Department of Chemical Engineering,University of California, Santa Barbara CA 93106-5130, USA

Received: 18 August 1997 / Received in final form: 1 December 1997 / Accepted: 2 December 1997

Abstract. We consider a planar interface between strongly-segregated homopolymers subjected to steady shear in the plane of the interface. We develop a constitutive equation for stress relaxation in an inhomogeneous system for chains obeying Rouse dynamics. Using this equation, the interfacial viscosity for a symmetric blend is found to be $\zeta b^2/(6\chi\nu_0)$ in agreement with a scaling prediction due to de Gennes, where ζ is the bead friction coefficient, b is the segment length, ν_0 is the segment volume and χ is the Flory-Huggins interaction parameter driving the phase separation. We generalize our results to asymmetric blends and describe a phenomenological extension to entangled melts.

PACS. 83.50.Lh Interfacial and free surface flows; slip – 83.80.Es Polymer blends

1 Introduction

There is currently much interest in slip phenomena in polymers [1–6]. Slip corresponds to a situation in which a polymeric material responds nonuniformly to an imposed shear stress, with the strain or rate of strain possessing spatial variations. Slip might reflect actual decohesion of a polymer with a solid substrate, *e.g.* a melt against a metal die, or simply smooth viscosity variations due to inhomogeneities in fluid microstructure or composition, *e.g.* a solution of non-absorbing polymers against a solid surface.

Studies on slip at polymer interfaces have generally been focused on "external" interfaces, such as homopolymer melts against air or solid surfaces. Here we consider a planar "internal" interface between two incompressible homopolymers, A and B. When the incompatibility between the two polymers (characterized by the Flory-Huggins parameter χ) is high, the system consists of almost pure bulk homopolymer phases separated by a thin interfacial region in which A and B mix.

If we shear such a blend parallel to the interface, we expect that the chain dynamics and segmental interactions in the interfacial region should profoundly affect the spatial distribution of shear. In particular, since the A-B interaction is repulsive, the interfacial viscosity ought to be lower than the bulk viscosity. The interface thus appears to "slip".

In the interest of simplicity, we begin by considering a symmetric blend (*i.e.* identical friction coefficients $\zeta_A = \zeta_B = \zeta$, statistical segment lengths $b_A = b_B = b$, segment volumes $\nu_A = \nu_B = \nu_0$ and degrees of polymerization $N_A = N_B = N$ for A and B), where the polymer chains obey Rouse dynamics [7]. A scaling result due to de Gennes [8] predicts that the interfacial viscosity is proportional to $1/\chi$. We should like to verify this result within a more quantitative analysis and extend the treatment to realistic cases of asymmetric blends.

In itself, this problem is relevant to the bulk processing of multi-phase polymer blends. From a broader perspective, it is part of a larger class of problems dealing with the dynamics of strongly inhomogeneous viscoelastic systems. The field of polymer rheology has historically been focused on homogeneous systems [7], while newer, "high-performance" types of polymeric systems such as block copolymers and blends [9] are manifestly inhomogeneous. Previous workers [10,11] have considered polymer solutions under shear where elastic stresses drive concentration fluctuations. They were concerned with deriving the dynamical equation for the polymer concentration, and used empirical constitutive relations to describe the polymer stress. Others [12–16] have explored further the coupling between stress and concentration for inhomogeneous systems, obtaining evolution equations for both the polymer stress and concentration. However, these analyses are only valid for inhomogeneities weak on the scale of the chain radius of gyration, R_g.

The inhomogeneity we consider here is both sharp compared to R_g, and of large amplitude (with respect to the concentration, which exhibits $O(1)$ variations through the interface[1]). We project a Fokker-Planck (FP) equation for the set of microscopic chain variables to equations of motion for the stress and concentration variables. We find

[a] e-mail: jlgoveas@mrl.ucsb.edu

[1] The chains themselves are not significantly perturbed from their random walk configurations, so the inhomogeneity with respect to say, chain stretching, is of small amplitude.

that while we can derive a completely general concentration equation, we must resort to a semi-phenomenological description for the stress relaxation. A necessary feature of this description is the coupling between gradients in stress and gradients in concentration. The case of the sheared blend is then a model problem (in that it is one-dimensional and the static limit is well-defined) for us to develop and test these constitutive equations, which we hope to apply quite generally to other strongly inhomogeneous systems.

This paper is organized as follows. In Section 2 we recapitulate the de Gennes scaling argument to which much of the rest of the paper is devoted to examining. Section 3 presents the statics of the blend due to Helfand and Tagami [17]. We derive the concentration and stress evolution equations in Sections 4 and 5, which we go on to apply to the symmetric sheared blend in Section 6 and consequently solve for the blend viscosity. We construct a simple physical model to explain these results in Section 7. This analysis is generalized to asymmetric blends in Section 8. In Section 9 we show how our formalism may be phenomenologically extended to entangled melts. We conclude in Section 10 with a discussion of extensions and related problems.

2 A scaling argument for the interfacial viscosity

Let us first consider a segregated, unentangled homopolymer blend at equilibrium, where the interfacial width $a_{\rm I}$ is large compared to the monomer length b, yet small compared to the radius of gyration of the chains, $R_{\rm g} \sim b(N/6)^{1/2}$. The interface consists mostly of loops of monomers that weave back and forth across the interface, and contains very few chain ends. A loop of s-monomers of A venturing into the pure B phase gains $k_{\rm B}T$ (which we set to unity) in entropy, offset by an enthalpic cost χs. The average loop length s^* then scales as $1/\chi$. Assuming Gaussian statistics for the loops, the interfacial width $a_{\rm I} \sim bs^{*1/2} \sim b/\chi^{1/2}$. (Thus in order for $b \ll a_{\rm I}$, we must have $\chi \ll 1$, and $a_{\rm I} \ll R_{\rm g}$ implies $\chi N \gg 1$).

Now subject such a blend to a simple shear flow. A homogeneous melt of A or B homopolymers exhibits a Rouse viscosity $\eta_0 \sim \zeta b^2 N/\nu_0$ [7]. De Gennes [8] argues that the viscosity in the A-B interfacial region is also given by a Rouse formula, but with N replaced by the average loop length, so that $\eta_i \sim \zeta b^2 s^*/\nu_0 \sim \zeta b^2/\chi\nu_0$.

It is not obvious to us why this formula should hold. While clearly the only scale in the interface is the loop length, one might imagine that stress relaxation of the loops in the interface is communicated to the rest of the chain in the bulk. In this paper we examine whether this scaling result for the interfacial viscosity is borne out by a more quantitative analysis.

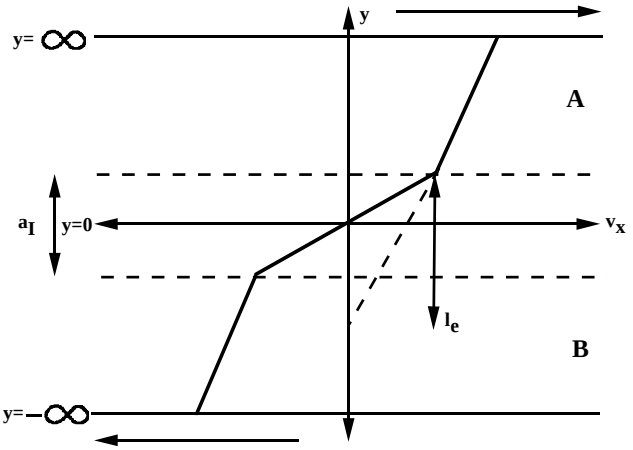

Fig. 1. Schematic showing the shear orientation for a strongly segregated blend, and the extrapolation length $l_{\rm e}$.

3 The equilibrium interface

We briefly review the results of a mean-field theory by Helfand and Tagami [17] for the static interface. Figure 1 shows the co-ordinate system we shall use: the dividing surface between the homopolymers is at $y = 0$, and the A and B monomer volume fractions $(\phi_{\rm A}, \phi_{\rm B})$ attain their bulk values of unity at $y = +\infty, -\infty$ respectively. The propagator $G_{\rm A}(y, y', s)$ (the probability density for a type-A chain of s-monomers to find itself at y' having started at y), becomes independent of the monomer-index s in the limit that the interface is sharp. This is the so-called "ground-state" approximation (see for example [18]). We define $Q_{\rm A}(y) = \int {\rm d}y' G_{\rm A}(y, y', s) = \phi_{\rm A}^{1/2}(y)$ which satisfies the equation

$$0 = \frac{b^2}{6}\frac{\partial^2 Q_{\rm A}}{\partial y^2} - U_{\rm A}(y) Q_{\rm A}. \tag{3.1}$$

The potential $U_{\rm A}(y)$ is written as $\chi\phi_{\rm B}(y) + \mu(y)$: the first term accounts for the repulsive interaction between A and B monomers, the second maintains melt incompressibility. An analogous equation for $Q_{\rm B}(y)$ together with the incompressibility condition $\phi_{\rm A}(y) + \phi_{\rm B}(y) = 1$, then forms a closed equation set that may be solved to give the unknown "pressure" field $\mu(y)$. The following results are obtained:

$$\phi_{\rm A}(y) = \frac{\exp[4y/a_{\rm I}]}{1 + \exp[4y/a_{\rm I}]} \tag{3.2}$$

$$a_{\rm I} = \frac{2b}{\sqrt{6\chi}} \tag{3.3}$$

$$U_{\rm A}(y) = \chi\phi_{\rm B}(1 - 3\phi_{\rm A}). \tag{3.4}$$

4 A constitutive equation for the stress

To study the dynamics of an inhomogeneous system, we shall adopt a mean-field picture and consider a single chain

in a potential $U(\mathbf{r},t)$. [For notational simplicity we temporarily suppress the species labels.] We project the FP equation for the probability distribution $\psi(\{\mathbf{R}\},t)$ of the set of microscopic chain variables $\{\mathbf{R}\}$ for an A chain, to equations for the two collective variables of interest: the monomer density and stress.

We begin with the FP equation for an A chain

$$\frac{\partial\psi(\{\mathbf{R}\},t)}{\partial t}=\int_0^N \mathrm{d}s\frac{\delta}{\delta\mathbf{R}(s)}\frac{1}{\zeta}\left[\frac{\delta}{\delta\mathbf{R}(s)}+\frac{\delta\mathcal{H}}{\delta\mathbf{R}(s)}\right]\psi(\{\mathbf{R}\},t) - \int_0^N \mathrm{d}s\frac{\delta}{\delta\mathbf{R}(s)}\cdot\mathbf{v}(\mathbf{R}(s),t)\psi(\{\mathbf{R}\},t) \quad (4.1)$$

where $\mathbf{v}(\mathbf{R}(s),t)$ is an external velocity field imposed on the system, assumed to be divergence-free (since the polymer melt is incompressible), and is determined such that the total shear stress is uniform. The time- and space-dependent Hamiltonian is defined by

$$\mathcal{H}(\{\mathbf{R}\},t)=\frac{3}{2b^2}\int_0^N \mathrm{d}s\left[\frac{\partial\mathbf{R}(s)}{\partial s}\right]^2 + \int_0^N \mathrm{d}s\; U(\mathbf{R}(s),t) \quad (4.2)$$

where the first term is due to chain stretching, and the second explicitly includes the system inhomogeneity through the external potential.

The volume fraction of A-monomers is defined as

$$\phi(\mathbf{r})=\mathcal{N}\nu_0\int_0^N \mathrm{d}s\int \mathrm{D}\{\mathbf{R}\}\psi\{\mathbf{R},\mathbf{t}\}\delta(\mathbf{r}-\mathbf{R}(\mathbf{s})) \quad (4.3)$$

where $\mathcal{N}$ is the number of A chains in the system. The stress supported by A-chains is defined by [7]

$$\sigma_{ij}(\mathbf{r})=\mathcal{N}\frac{3}{b^2} \times\int_0^N \mathrm{d}s\int \mathrm{D}\{\mathbf{R}\}\psi(\{\mathbf{R}\},t)\dot{R}_i(s)\dot{R}_j(s)\delta(\mathbf{r}-\mathbf{R}(s)) \quad (4.4)$$

where the $i-j$th component of the stress tensor $\boldsymbol{\sigma}$ is given by σ_{ij}, and dots indicate derivatives with respect to s.

Multiplying equation (4.1) by $\delta(\mathbf{r}-\mathbf{R}(s))$ and integrating over $\int_0^N \mathrm{d}s\int D\{\mathbf{R}\}$ gives the concentration equation. After several integrations by parts we get

$$\frac{\partial\phi}{\partial t}=-\boldsymbol{\nabla}\cdot\mathbf{J}=-\mathbf{v}\cdot\boldsymbol{\nabla}\phi+\frac{1}{\zeta}\boldsymbol{\nabla}\cdot(\phi\boldsymbol{\nabla}U) + \frac{1}{\zeta}\nabla^2\phi-\frac{\nu_0}{\zeta}\boldsymbol{\nabla}\boldsymbol{\nabla}:\boldsymbol{\sigma} \quad (4.5)$$

where $\mathbf{J}$ is the concentration flux. [Note that the boundary terms vanish for $\{\mathbf{R}\}$ integrations because configurations that involve the chain being completely extended have very low probability, and for s-integrations because there is no tension on free chain ends.]

The first term in equation (4.5) is the explicit coupling of the flow-field to the concentration. The next term is due to the external potential; the third term arises from the Brownian force and the last term describes the effects of the chain elastic forces.

At equilibrium (*i.e.* in the absence of flow, $\mathbf{v}=0$) the concentration flux must be zero

$$\phi\boldsymbol{\nabla}U=\boldsymbol{\nabla}\cdot(\boldsymbol{\sigma}\nu_0-\boldsymbol{\delta}\phi) \quad (4.6)$$

(where $\boldsymbol{\delta}$ is the unit tensor) showing simply that the elastic forces balance the potential forces. This equation thus provides a condition on what the stress must reduce to in equilibrium, which we shall use shortly. We may also express equation (4.6) as $\phi\boldsymbol{\nabla}U=\nu_0\boldsymbol{\nabla}\cdot\boldsymbol{\Sigma}$, where $\boldsymbol{\Sigma}$ is the deviatoric stress *i.e.* the difference between the stress and its value in the absence of any external fields:

$$\boldsymbol{\Sigma}=\boldsymbol{\sigma}-\boldsymbol{\delta}\phi/\nu_0. \quad (4.7)$$

By a similar procedure, we obtain a constitutive equation for the stress (multiplying by $\dot{R}_i(s)\dot{R}_j(s)\delta(\mathbf{r}-\mathbf{R}(s))$ instead)

$$\begin{aligned}\partial_t\sigma_{ij} =& -v_k\nabla_k\sigma_{ij}+(\nabla_k v_i)\sigma_{kj}+\sigma_{ki}\nabla_k v_j \\ &+\frac{1}{\zeta}\nabla_k(\nabla_k U\sigma_{ij})-\frac{1}{\zeta}(\nabla_i\nabla_k U)\sigma_{kj} \\ &-\frac{1}{\zeta}(\nabla_j\nabla_k U)\sigma_{ki}+\{\mathcal{NS}\}_{ij}. \end{aligned} \quad (4.8)$$

Here the first and second lines arise from the flow-field and external potential, respectively. By $\{\mathcal{NS}\}_{ij}$ we wish to denote the terms that contribute to the stress relaxation due to the noise and stretching. Formally these are written as

$$\begin{aligned}\{\mathcal{NS}\}_{ij} =& \frac{1}{\zeta}\nabla^2\sigma_{ij} \\ &+\frac{1}{\zeta}\left(\frac{3}{b^2}\right)\left[-2\int \mathrm{d}s\langle\ddot{R}_i\ddot{R}_j\delta(\mathbf{r}-\mathbf{R}(s))\rangle\right. \\ &-2\nabla_k\int \mathrm{d}s\langle\dot{R}_i\dot{R}_j\ddot{R}_k\delta(\mathbf{r}-\mathbf{R}(s))\rangle \\ &\left.+\nabla_k\nabla_l\int \mathrm{d}s\langle\dot{R}_i\dot{R}_j\dot{R}_k\dot{R}_l\delta(\mathbf{r}-\mathbf{R}(s))\rangle\right] \end{aligned} \quad (4.9)$$

where $\langle\cdot\rangle$ denotes the non-equilibrium average $\int \mathrm{D}\{\mathbf{R}\}\psi\{\mathbf{R}\}(\cdot)$. Since the averages above contain terms higher order than $\dot{R}_i\dot{R}_j$, they prove to be difficult to calculate exactly.

One approach to evaluating these averages, under weak shear conditions, is to make the local equilibrium approximation. This is a scheme developed by Kawasaki and Sekimoto [19] where a set of hydrodynamic variables (in this case the monomer density and the stress) are assumed to be the only slow variables. The microscopic variables consequently relax quickly to their local equilibrium values, such that the hydrodynamic variables take on certain constrained values. For example, keeping the stress and

concentration as the slow variables leads to the following stress evolution equation

$$\frac{\partial \sigma_{ij}(\mathbf{r})}{\partial t} = -\int \mathrm{d}\mathbf{r}' \Lambda^{\sigma\sigma}_{ijkl}(\mathbf{r}\mathbf{r}') \frac{\partial \mathcal{H}}{\partial \sigma_{kl}(\mathbf{r}')} - \int \mathrm{d}\mathbf{r}' \Lambda^{\sigma\phi}(\mathbf{r}\mathbf{r}') \frac{\partial \mathcal{H}}{\partial \phi(\mathbf{r}')} \quad (4.10)$$

where the $\Lambda^{pq}(\mathbf{r}\mathbf{r}')$'s constitute a matrix of projected Onsager coefficients and are defined as

$$\Lambda^{pq}(\mathbf{r}\mathbf{r}') = \langle \frac{\delta \hat{p}(\mathbf{r})}{\delta \mathbf{R}} \cdot \hat{\Lambda}(\mathbf{R}) \cdot \frac{\delta \hat{q}(\mathbf{r}')}{\delta \mathbf{R}} \rangle_{\{p,q\}}. \quad (4.11)$$

Here $\hat{\Lambda}(\mathbf{R})$ is the microscopic matrix of kinetic coefficients, and is equal to $(1/\zeta)\boldsymbol{\delta}$ for Rouse chains. The hatted quantities are microscopic densities (here, the concentration and stress), and the average is now an *equilibrium* average with $\hat{p}$ and $\hat{q}$ constrained to be p and q respectively. Performing this procedure yields equations for the monomer density and stress identical to equations (4.5, 4.8), except that the non-equilibrium averages are replaced by constrained equilibrium averages.

Thus it is clear that within a local equilibrium approximation, the noise-stretch terms $\{\mathcal{NS}\}_{ij}$ in equation (4.8) can be expressed as functionals of σ_{ij} and ϕ. In the next section, we shall use this fact to guess the form of these terms.

5 An approximate stress constitutive equation

Let us construct an approximation for the noise and stretching terms in equation (4.8). Our first observation is that at *equilibrium*, these terms in equation (4.8) must exactly cancel the potential terms, *i.e.* the U-dependent terms. For a sharp interface, U is explicitly[2] $O(\chi)$, with each derivative contributing a factor of $1/a_\mathrm{I} \sim \sqrt{\chi}$, so that all three potential terms are $O(\chi^2)$. Furthermore, by inspection of equation (4.6), it is evident that

$$\boldsymbol{\sigma} = (\phi/\nu_0)\boldsymbol{\delta} + O(\chi). \quad (5.1)$$

Thus, at leading order (for $\chi \ll 1$), the potential terms can be transformed by setting $\sigma_{ij} \approx (\phi/\nu_0)\delta_{ij}$ and $\nabla_i U \approx (\nu_0\phi^{-1})\nabla_k \Sigma_{ik}$, into terms involving only $\phi, \nabla\phi$ and gradients of $\boldsymbol{\Sigma}$. Since at equilibrium these terms must cancel $\{\mathcal{NS}\}_{ij}$, they can correspond to $-\{\mathcal{NS}\}_{ij}$. To this end we write

$$\{\mathcal{NS}\}_{ij} \approx -\frac{6}{\zeta {R_\mathrm{g}}^2}\Sigma_{ij} + \frac{1}{\zeta}[\nabla_i\nabla_j\Sigma_{jk} + \nabla_j\nabla_k\Sigma_{ik} - \delta_{ij}\nabla_k\nabla_l\Sigma_{kl}] - \frac{1}{\zeta\phi}[\nabla_i\phi\nabla_k\Sigma_{jk} + \nabla_j\phi\nabla_k\Sigma_{ik}]. \quad (5.2)$$

Note that the first term is not obtained by the procedure outlined above[3], but was added by hand to account for the long-time stress relaxation in a *homogeneous* melt. The numerical factor of $\boldsymbol{\Sigma}$ is chosen to exactly reproduce the bulk Rouse viscosity. (See Sect. (6.3) for a comparison of our stress constitutive equation with the Maxwell approximation.)

A few comments about equation (5.2) are in order. The second group of terms involves two gradients of $\boldsymbol{\Sigma}$, and *resembles* the term $\nabla^2\boldsymbol{\Sigma}/\zeta$ derived by other workers [12–16] (see [20] for a comparison of these different formalisms), based on long-wavelength gradient expansions, *i.e.* scales larger than R_g. The crucial assumptions made in these analyses (with the exception of [13]) are that the chain distribution function may be expanded around the center of mass, and that the chain may be modelled as a Hookean dumbell (*i.e.* only the first Rouse mode is kept). In contrast, here we assume that $\chi \ll 1$ and adopt a local equilibrium approximation.

Notice however, that even when $a_\mathrm{I} \sim R_\mathrm{g}$, U is still $O(\chi)$. For $a_\mathrm{I} \gg b$, we must have[4] $\chi \ll 1$, so that the arguments leading to the derivation of equation (5.2) are still valid. This means that the tensorial form of the stress gradient terms in equation (5.2) continues to hold in the long-wavelength limit. We submit that the structural differences between these gradient terms and those in references [12–16] are a consequence of the dumbell approximation and localization of stress at the center of mass in these earlier works.

The terms involving $\boldsymbol{\nabla}\phi$ and $\boldsymbol{\nabla}\boldsymbol{\Sigma}$ describe the coupling between stress and concentration gradients in an inhomogeneous system. (Note that these terms are absent in the stress constitutive equations of references [12–16], even though they are in principle of the same order, even in the long-wavelength limit.) Equation (5.2) shows that stress gradients can still exist in the absence of concentration gradients. As an example of such a situation, we might imagine preparing an initial condition of non-uniform chain stretching in a one-phase melt, and ask how the stress relaxes in this case.

We have neglected higher order gradients in $\boldsymbol{\Sigma}$ and ϕ, which is a good approximation in the typical situation when $\chi \ll 1$. (However, there may be other inhomogeneous systems where these higher order terms become important. Also, since Eq. (5.2) is derived using a local equilibrium criterion, in principle other terms may appear at high shear rates. We shall show in Sect. 6.2 that Eq. (5.2) also holds far from equilibrium.)

In closing this section, we summarize our approximate constitutive equation for a Rouse chain in an external

[2] Of course the results of Section 3 only apply to a one-dimensional interface, but the scaling results are easily generalized to higher dimensions. The three dimensional analog of equation (3.4) is $0 = (b^2/6)\nabla^2 Q - U(\mathbf{r})Q$. Recall that $U(\mathbf{r}) = \chi\phi_\mathrm{A}(\mathbf{r}) + \mu(\mathbf{r})$, so $U(\mathbf{r})$ is $O(\chi)$ (since the potential that maintains incompressibility is of the same order as the A-B interaction potential). Balancing the potential term against the gradient terms gives $1/a_\mathrm{I}^2 \sim O(\chi)$.

[3] At equilibrium, this term is $(1/\chi N)$ times smaller than the other terms and may be dropped.

[4] When $a_\mathrm{I} \sim R_\mathrm{g}$ however we may no longer use the ground-state approximation.

potential:

$$\partial_t\sigma_{ij} = -v_k\nabla_k\sigma_{ij} + (\nabla_k v_i)\sigma_{kj} + \sigma_{ki}\nabla_k v_j + \frac{1}{\zeta}\nabla_k(\nabla_k U\sigma_{ij}) - \frac{1}{\zeta}(\nabla_i\nabla_k U)\sigma_{kj} - \frac{1}{\zeta}(\nabla_j\nabla_k U)\sigma_{ki} + \frac{6}{\zeta {R_g}^2}\Sigma_{ij} + \frac{1}{\zeta}[\nabla_i\nabla_k\Sigma_{jk} + \nabla_j\nabla_k\Sigma_{ik} - \delta_{ij}\nabla_k\nabla_l\Sigma_{kl}] - \frac{1}{\zeta\phi}[\nabla_i\phi\nabla_k\Sigma_{jk} + \nabla_j\phi\nabla_k\Sigma_{ik}]. \quad (5.3)$$

6 Interfacial viscosity of a symmetric blend

6.1 General equations for the one-dimensional case

We now apply the results of the previous section directly to the sheared blend. The position-dependent viscosity of the blend is defined as $\eta(y) = \sigma_0/\kappa(y)$, where σ_0 is the applied stress and $\kappa(y) = \partial v_x/\partial y$ is the shear rate, with v_x denoting the x-component of the velocity.

To determine the shear rate, in general we must solve a set of coupled differential equations for the stress and density fields. At steady-state, the xy-component of the equation for the A-stress (from Eq. (5.3)) is given by

$$0 = \kappa(y)\sigma_{yy} + \frac{1}{\zeta}U'\sigma'_{xy} - \frac{6}{\zeta {R_g}^2}\sigma_{xy} - \frac{1}{\zeta}\frac{\phi'}{\phi}\sigma'_{xy} + \frac{1}{\zeta}\sigma''_{xy}. \quad (6.1)$$

Primes indicate differentiation with respect to y. The corresponding equation for σ_{yy} is

$$0 = \frac{1}{\zeta}\left[U'\sigma'_{yy} - U''\sigma_{yy} - \frac{6}{R_g^2}\Sigma_{yy} - 2\frac{\phi'}{\phi}\Sigma'_{yy} + \Sigma''_{yy}\right]. \quad (6.2)$$

The A-density equation from (4.5) is

$$0 = \frac{1}{\zeta}[(-\phi U') + (\sigma_{yy}{}'\nu_0 - \phi')]'. \quad (6.3)$$

There are three analogous equations for the B-species.

These equations must be solved under the constraints that the total monomer density and shear stress are maintained constant everywhere, *i.e.* $\phi_A + \phi_B = 1$ and $\sigma_{A,xy} + \sigma_{B,xy} = \sigma_0$, respectively. Far away from the interface, the system consists of bulk homopolymer phases *i.e.* $\phi_A(+\infty) = \phi_B(-\infty) = 1$ and $\sigma_{A,xy}(+\infty) = \sigma_{B,xy}(-\infty) = \sigma_0$, and we recover the Rouse viscosity so that $\kappa(-\infty) = \kappa(+\infty) = \kappa_0 = 6\sigma_0\nu_0/\zeta {R_g}^2$ [7]. Altogether this gives eight equations for the eight unknowns $\sigma_{A,xy}, \sigma_{B,xy}, \sigma_{A,yy}, \sigma_{B,yy}, \phi_A, \phi_B, \kappa(y)$ and $\mu(y)$ (where we recall that $\mu(y)$ is the part of $U(y)$ common to A and B that maintains incompressibility).

6.2 Solution of coupled equations

Integrating equation (6.3) over y with the boundary conditions that at $y \to -\infty, +\infty$ all gradients in U, ϕ and σ_{yy} vanish gives

$$0 = -(\phi U') + (\nu_0\sigma_{yy}{}' - \phi') \quad (6.4)$$

which is identical with the equilibrium condition, equation (4.6). Integrating this equation a second time gives $\nu_0\sigma_{yy} = \phi + \int_{-\infty}^{y} \mathrm{d}y'\phi U'$ (where we have used the boundary conditions $\sigma_{yy} = 0$ and $\phi = 0$ at $y = -\infty$), which may be used to eliminate σ_{yy} from equation (6.1). This xy-stress equation may then be solved for the shear rate under the constraint of uniform total shear stress.

Notice that the equilibrium concentration and potential profile given by equations (3.2) and (3.4) respectively, are steady-state solutions to the equation set of the previous section at *all* shear rates. This is a consequence of the absence of explicit coupling to the flow-field in the yy-stress equation. [This is a peculiarity of the Rouse model, for which the second-normal stress difference [7] in a homogeneous melt is always zero (and therefore independent of the shear rate), even at high shear rates.] This supports the application of equation (5.2) far from equilibrium because the concentration profile takes its equilibrium value at all shear rates, so that $\nabla \sim (1/\chi)$ and higher order gradient terms are negligible for $\chi \ll 1$.

Overall, we see that equations (6.3, 6.2) for the A and B species, together with the constant density constraint give five equations for the five unknowns $\sigma_{yy,A}$, $\sigma_{yy,B}, \phi_A, \phi_B, \mu(y)$, which are decoupled from the shear stress equations and constant shear stress constraint. Thus, neglecting terms of $O(\chi)$, we can set $\sigma_{yy} \approx \phi/\nu_0$ in equation (6.1).

We see from equation (6.1) that the term coupling stress gradients and concentration gradients comes into play only on the scale of the interface (since $\phi' \sim 1/a_I$). The stress-gradient term persists up to a distance on the order of the radius of gyration of the chain, but this provides only exponentially small corrections to the stress profile on the scale of the interface. Beyond R_g, the bulk homopolymer dynamics are recovered. Thus, for $y \gg a_I$ the dominant balance in equation (6.1) is between the first and third terms, which gives the Rouse result $\eta_0 \sim \zeta R_g^2/\nu_0$. Instead, for $y \sim a_I$, the balance is between the flow term and the two gradient terms, which gives $\eta_i \sim \zeta a_I^2/\nu_0$. Thus, we see that the scaling ideas of [8] are in fact borne out.

Let us next rewrite equation (6.1) in terms of a new variable $T_A = \sigma_{A,xy} - \sigma_0\phi_A$

$$0 = g(y) - \frac{6}{\zeta {R_g}^2}T_A - \frac{1}{\zeta}\frac{\phi_A{}'}{\phi_A}T_A{}' + \frac{1}{\zeta}T_A{}'' \quad (6.5)$$

where the inhomogeneous term is given by

$$g(y) = (\kappa - \kappa_0)\frac{\phi_A}{\nu_0} - \frac{\sigma_0}{\zeta}\left[\frac{(\phi_A{}')^2}{\phi_A} - \phi_A{}''\right] \quad (6.6)$$

and ϕ_A is given by equation (3.2). (Note that the potential term may be dropped because it is a factor of χ smaller than the other terms). The boundary conditions are $T_A \to 0, T_B \to 0$ for $y \to \infty$, and $T_A \to 0, T_B \to 0$ for $y \to -\infty$ (T_B being defined similarly to T_A).

We now construct a Green's function $G_{\rm A}(y,a)$ for equation (6.5) so that

$$T_{\rm A}(y) = -\int_{-\infty}^{\infty} {\rm d}a\, g(a) G_{\rm A}(y,a). \tag{6.7}$$

The condition of constant shear stress is then given by

$$\begin{aligned} 0 &= T_{\rm A}(y) + T_{\rm B}(y) \\ &= \int_{-\infty}^{\infty} {\rm d}a\, g(a)[G_{\rm A}(y,a) + G_{\rm B}(y,-a)] \end{aligned} \tag{6.8}$$

where we have defined a similar Green's function for B, and used the symmetry $\phi_{\rm B}(y) = \phi_{\rm A}(-y)$ in deriving equation (6.8). This equation has the solution $g(a) = 0$ so that

$$\kappa(y) = \kappa_0 + \frac{\sigma_0 \nu_0}{\zeta} \left(\frac{4}{a_{\rm I}}\right)^2 \phi_{\rm A}\phi_{\rm B}. \tag{6.9}$$

This means that $T_{\rm A}(y) = 0, T_{\rm B}(y) = 0$, so that $\sigma_{{\rm A},xy} = \sigma_0 \phi_{\rm A}$ (and similarly for B), *i.e.* that the stress supported by the A-chains is directly proportional to the concentration of A-chains. However this simple result does not carry over to the non-symmetric blend (see Sect. 8). The blend viscosity is thus given by

$$\begin{aligned} \eta(y) &= \frac{\sigma_0}{\kappa_0 + \dfrac{\sigma_0 \nu_0}{\zeta}\left(\dfrac{4}{a_{\rm I}}\right)^2 \phi_{\rm A}\phi_{\rm B}} \\ &= \frac{\zeta a_{\rm I}^2}{\dfrac{\nu_0}{6}\left(\dfrac{a_{\rm I}}{R_{\rm g}}\right)^2 + 4^2 \phi_{\rm A}\phi_{\rm B}\nu_0} \end{aligned} \tag{6.10}$$

which reduces to the Rouse viscosity in the bulk, and gives in the interface

$$\eta_i(y) \approx \left(\frac{a_{\rm I}}{4}\right)^2 \frac{\zeta}{\phi_{\rm A}\phi_{\rm B}\nu_0} \tag{6.11}$$

The characteristic scale for the interfacial viscosity is set at $y = 0$ to be $\zeta b^2/(6\chi\nu_0)$.

6.3 Comparison to the Maxwell model

We should point out an important difference between our constitutive equation and the Maxwell model [21], a widely used empirical constitutive equation for homogeneous systems

$$\frac{{\rm D}\boldsymbol{\sigma}}{{\rm D}t} - (\boldsymbol{\nabla}\mathbf{v})^{\rm T} \cdot \boldsymbol{\sigma} - \boldsymbol{\sigma} \cdot \boldsymbol{\nabla}\mathbf{v} + \frac{1}{\tau}(\boldsymbol{\sigma} - G_{\rm e}\boldsymbol{\delta}) = 0 \tag{6.12}$$

where $D/Dt = \partial/\partial t + \mathbf{v}\cdot\boldsymbol{\nabla}$ is the convected time derivative, τ is the rheological relaxation time and $G_{\rm e}$ is the shear modulus. For the Rouse model, the longest relaxation time is given by $\tau \sim N^2$ and $G_{\rm e} \sim \phi/N$ [7]. For a steady simple shear flow, the xy-component of equation (6.12) is

$$0 = \kappa\sigma_{yy} - \frac{1}{\tau}\sigma_{xy}. \tag{6.13}$$

The yy-component of the stress equation gives $\sigma_{yy} = G_{\rm e}$, which upon substituting into equation (6.13) gives the bulk Rouse viscosity $\sim N$. Notice that the coefficient of the σ_{xy} term in the Maxwell model is $1/N$ times smaller than the coefficient we have used in equation (6.1). This is a consequence of the fact that we take the homogeneous equilibrium isotropic stress to be proportional to ϕ, whereas the Maxwell model takes it to be proportional to ϕ/N. On physical grounds, one does not expect the isotropic stress to depend on the length of the polymer chains. Indeed, the N-dependence of the isotropic stress in the Maxwell model is an artifact of truncating the spectrum of relaxation times.

6.4 Apparent blend viscosity

Let us now define a quantity called the "extrapolation length" [8], which is a measure of the deviation of the interfacial velocity from the bulk linear velocity profile. Integrating equation (6.9) for the shear rate gives the velocity profile

$$v_x = \kappa_0 y + \frac{\nu_0\sigma_0}{\zeta}\frac{4}{a_{\rm I}}\left[\phi_{\rm A} - \frac{1}{2}\right]. \tag{6.14}$$

The extrapolation length, $l_{\rm e}$, is given by the value of y where v_x extrapolates back to zero (see Fig. 1). This is given by the outer limit of equation (6.14), obtained by replacing $\phi_{\rm A}(y) \to 1$. For the symmetric Rouse blend, we find

$$\begin{aligned} |l_{\rm e}| &= \frac{R_{\rm g}^2}{3\,a_{\rm I}} = \sqrt{\frac{\chi}{6}}\frac{R_{\rm g}^2}{b} \\ &\sim a_{\rm I}\frac{\eta_0}{\eta_i}. \end{aligned} \tag{6.15}$$

For a system of finite size L, with an interface present, the apparent shear rate is given by (see Fig. 2)

$$\kappa_{\rm app} = \frac{\Delta v}{L} = \kappa_0\left[1 + \frac{2l_{\rm e}}{L}\right]. \tag{6.16}$$

The apparent viscosity is then

$$\eta_{\rm app} = \frac{\eta_0}{\left[1 + \dfrac{2l_{\rm e}}{L}\right]}. \tag{6.17}$$

The interface then only makes itself felt in terms of the rheological properties if $l_{\rm e} \gg L$. For $\chi \approx 0.1$, $b \approx 3$ Å, $N \approx 100$, we get an extrapolation length on the order of Angstroms. For a bulk blend with a single interface, the interfacial slip does not significantly affect the measured viscosity, since the system size is usually many times the extrapolation length.

However, for multi-layered system like laminates, the layer size can fall below micron scales. (The apparent viscosity of a laminate is given by Eq. (6.17) because both the "velocity jump" and the system size are linear in the number of layers.) A more remarkable case is an entangled

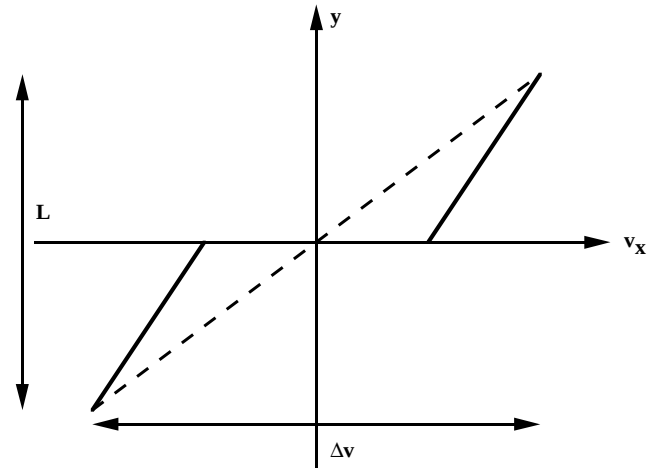

Fig. 2. The apparent viscosity of the blend is given by the slope of the dotted line, while the slope of the solid lines reflects the bulk viscosity. The "velocity" jump is denoted by Δv, and the system size by L.

melt where Rouse-like friction dominates in the interface (see Sect. 9). Here, the extrapolation length is much larger than that for the Rouse melt (since η_0 in Eq. (6.15) is replaced by the viscosity of an entangled melt). For multilayered systems like laminates where the layer size can fall below micron scales, this extrapolation length can be many times the layer size, so that the apparent viscosity can be significantly lower than the homopolymer bulk viscosity.

7 A "cartoon" for explaining the interfacial viscosity

Now we use the results of the previous section to give a simple physical picture of the dynamics of a blend under shear. First, we consider the case of a bulk Rouse melt, which we then compare with a segregated symmetric blend.

7.1 Bulk Rouse viscosity

Consider a Rouse melt under simple steady shear (see Fig. 3), such that $v_x = \kappa_0 y$. Let us focus our attention on a chain with its center of mass (c.o.m.) at $y = 0$. On average, this chain is stationary *i.e.* $v_{\rm c.o.m} = 0$. There is thus a drag along the entire length of the chain, due to the difference between the velocity of the surrounding fluid (made up of all the other chains in the melt) and the chain velocity. Since there is no hydrodynamic interaction between monomers, the drag coefficient for a length of n monomers is simply $n\zeta$. Thus the drag on the upper half of the chain is

$$\mathbf{F}_{\rm drag} \sim \hat{\mathbf{x}}(\kappa_0 R_{\rm g} - v_{\rm c.o.m.}) \left(\frac{N\zeta}{2}\right). \tag{7.1}$$

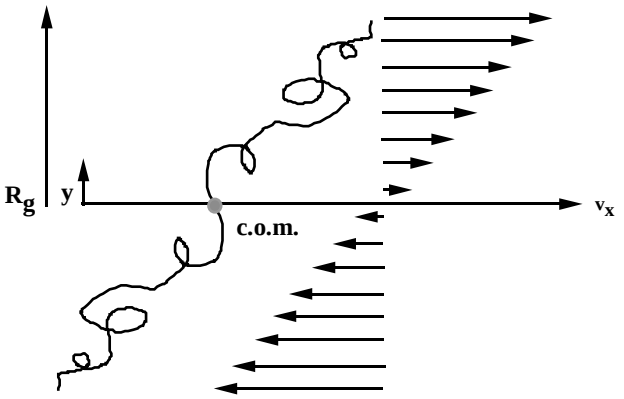

Fig. 3. A typical chain in a homogeneous Rouse melt under shear, is subjected to a drag force from the surrounding chains along its entire length.

The drag on the lower half of the chain is equal and opposite, so the tension on the monomers crossing the $y = 0$ plane is

$$\tau \sim \kappa_0 R_{\rm g} N\zeta. \tag{7.2}$$

The number of chains per unit area within $R_{\rm g}$ of the interface is $R_{\rm g}/\nu_0 N$. The shear stress is then

$$\sigma_{xy} \sim \tau(R_{\rm g}/N\nu_0) \sim \kappa_0 \zeta R_{\rm g}^2/\nu_0 \tag{7.3}$$

which gives the Rouse viscosity

$$\eta = \frac{\sigma_{xy}}{\kappa_0} \sim \zeta R_{\rm g}^2/\nu_0. \tag{7.4}$$

7.2 Interfacial viscosity

As we discussed in Section 2, the configuration of chains in the interface of a strongly-segregated blend consists mostly of loops. This is a fundamentally different picture from the previous section, because the chain center of mass is now significantly displaced from the interface symmetry plane (see Fig. 4). The drag on most of the monomers of the chain is small, since the chain (moving at the c.o.m. velocity) is simply convected along with the flow. The fluid in the interface, however, is almost stationary, so that there is a larger drag on the monomers in the interface (which are also moving with the velocity of the c.o.m).
Let us write an approximate velocity profile through the melt as

$$\begin{aligned} v_x(y) &= \kappa_i y && y \le a_{\rm I} \\ &= \kappa_i a_{\rm I} + \kappa_0 (y - a_{\rm I}) && y > a_{\rm I} \end{aligned} \tag{7.5}$$

where we assume the existence of a length scale $a_{\rm I}$, but do not say anything *a priori* about the "interfacial" shear rate κ_i. The velocity of the c.o.m. is then $v_x(R_{\rm g}) \approx \kappa_i a_{\rm I} + \kappa_0 R_{\rm g}$. A loop in the interface composed of s^* monomers (see Fig. 4) is subjected to drag forces from fluid moving at equal and opposite velocities on either side of the interface

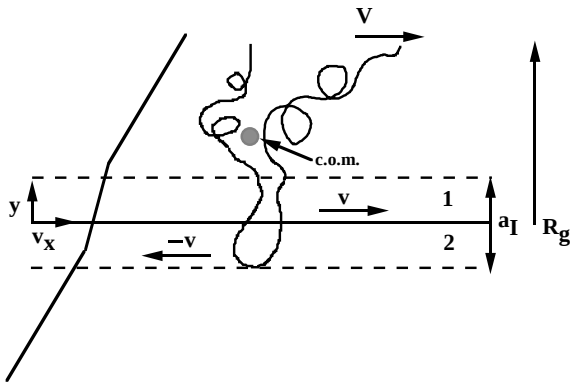

Fig. 4. Typical configurations of chains in the interface are loops. Under shear, the drag on chains in the interface, from the surrounding fluid, is mostly exerted on the monomers of these loops.

symmetry plane. The drag force on the upper half of the loop is

$$\mathbf{f}_1 \sim \hat{\mathbf{x}}(v_i - v_{\text{c.o.m.}})\frac{\zeta s^*}{2} \tag{7.6}$$

where $v_i \sim \kappa_i a_\text{I}$. The drag on the lower half of the loop is

$$\mathbf{f}_2 \sim \hat{\mathbf{x}}(-v_i - v_{\text{c.o.m.}})\frac{\zeta s^*}{2}\cdot \tag{7.7}$$

The total drag on a loop in the interface is then given by

$$\mathbf{F}_\text{drag} = \mathbf{f}_1 + \mathbf{f}_2 \sim \hat{\mathbf{x}} v_{\text{c.o.m.}}\zeta s^*. \tag{7.8}$$

Consequently, the tension on a loop is

$$\tau \sim v_{\text{c.o.m.}}\zeta s^* \sim [\kappa_i a_\text{I} + \kappa_0 R_\text{g}]\zeta s^*. \tag{7.9}$$

Since there are $a_\text{I}/\nu_0 s^*$ loops per area of interface, the total shear stress is given by

$$\sigma_{xy} \sim [\kappa_i a_\text{I} + \kappa_0 R_\text{g}]\zeta a_\text{I}/v_0. \tag{7.10}$$

The interfacial viscosity is therefore

$$\eta_i = \frac{\sigma_{xy}}{\kappa_i} \sim \frac{\zeta {a_\text{I}}^2}{\nu_0}\left[1 + \frac{\kappa_0}{\kappa_i}\frac{R_\text{g}}{a_\text{I}}\right]. \tag{7.11}$$

Since the total shear stress is constant, $\kappa_i\eta_i \sim \kappa_0\eta_0$, equation (7.11) can be expressed as an implicit equation for η_i that may be solved to give

$$\eta_i \sim \frac{\zeta {a_\text{I}}^2}{\nu_0}\left[1 + O\left(\frac{a_\text{I}}{R_\text{g}}\right)\right] \sim \frac{\zeta}{\chi\nu_0}\cdot \tag{7.12}$$

If we had considered the A-stress instead of the total stress, the arguments above would be unchanged, except that the number of loops supporting the stress would vary as the concentration through the interface. Thus $\sigma_\text{A} \propto \phi_\text{A}$, precisely as we found in Section 6.2.

8 Asymmetric blends

In the case that the homopolymers are not symmetric (*i.e.* that they have different degrees of polymerization or friction coefficients), equation (6.8) must be replaced by

$$0 = \int_{-\infty}^{\infty} \mathrm{d}a[S(a,y)\kappa(a)] + h(y) \tag{8.1}$$

where

$$S(a,y) = -\frac{1}{\sigma_0\nu_0}\left[\zeta_\text{A}\phi_\text{A}G_\text{A}(a,y) + \zeta_\text{B}\phi_\text{B}G_\text{B}(a,y)\right] \tag{8.2}$$

$$h(y) = \int_{-\infty}^{\infty}\left\{\left[\zeta_\text{A}\phi_\text{A}\frac{\kappa_{0,\text{A}}}{\sigma_0\nu_0} + \left(\frac{4}{a_\text{I}}\right)^2\phi_\text{A}^2\phi_\text{B}\right]G_\text{A}(a,y) + \left[\zeta_\text{B}\phi_\text{B}\frac{\kappa_{0,\text{B}}}{\sigma_0\nu_0} + \left(\frac{4}{a_\text{I}}\right)^2\phi_\text{A}\phi_\text{B}^2\right]G_\text{B}(a,y)\right\} \tag{8.3}$$

where $\kappa_{0,\text{A}} = 6\sigma_0\nu_0/\zeta_\text{A}R_{\text{g,A}}^2$ and $\kappa_{0,B} = 6\sigma_0\nu_0/\zeta_\text{B}R_{\text{g,B}}^2$. (We show how to construct the Green's functions for the above equation in Appendix A.) This is an inhomogeneous Fredholm equation of the first kind that must be solved numerically for the shear rate $\kappa(y)$. The discrete form of the integral equation can be written as a matrix equation

$$\mathbf{S}\cdot\boldsymbol{\kappa} = \mathbf{h} \tag{8.4}$$

where we use a Gauss-Legendre quadrature scheme to obtain the discretization points for the integration range. $\kappa(y)$ may then be easily obtained by inverting the matrix $\mathbf{S}$.

Figure 5 shows $\kappa(y)/(\sigma_0\nu_0)$ for an asymmetric blend with $\chi = 0.1, \zeta_\text{A} = 1, w = \zeta_\text{A}/\zeta_\text{B} = 0.5, R_{g,\text{A}} = R_{g,\text{B}} = 9a_\text{I}$. Notice that the peak in the shear rate is shifted over towards the more easily sheared B-species. We find that the position of this peak is only a function of w (holding $R_{\text{g,A}} = R_{\text{g,B}}$ constant), such that $f(w) = -f(1/w)$ due to symmetry. We also plot $T_\text{A}/\sigma_0 = \sigma_{xy,\text{A}}/\sigma_0 - \phi_\text{A}$ for the same blend in Figure 6, which is now non-zero in contrast to the symmetric case, so that the A-shear stress no longer tracks the A-monomer density profile. The "cartoon" of Section 7.2 requires that the shear rate is symmetrical around zero (since the A-density variation is not incorporated precisely), so that it cannot be used to capture these details of the asymmetric blend.

However, we can generalize the scaling results of Section 7.2. Let us write the interfacial viscosity (defined as the minimum viscosity in the blend) for an asymmetric blend (with $R_{\text{g,A}} = R_{\text{g,B}}$) as

$$\eta_i \approx (\zeta_\text{A}\zeta_\text{B})^{1/2}\frac{{a_\text{I}}^2}{\nu_0}F(w) + \eta_{i,\text{sym}} \tag{8.5}$$

where $\eta_{i,\text{sym}}$ is given by equation (6.10), $F(w) = F(1/w)$ by symmetry, and $F(1) = 0$. In Figure 7, we plot $F(w)$ for four blends with different values of R_g/a_I. We find that while $F(w)$ is not a universal function due to a slight

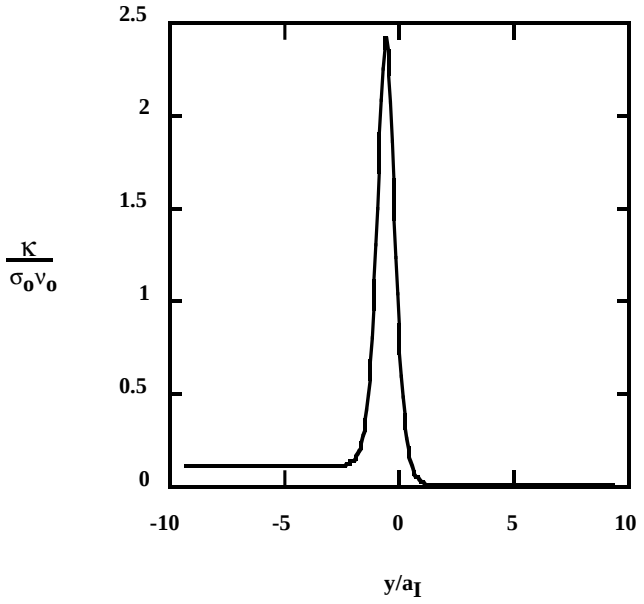

Fig. 5. $\kappa(y)/(\sigma_0\nu_0)$ for an asymmetric blend with $\chi = 0.1, \zeta_A = 1, w = \zeta_A/\zeta_B = 0.5, R_{g,A}/a_I = R_{g,B}/a_I = 9$. The maximum in the shear rate $\kappa(y)$ is shifted towards the more easily sheared B-species.

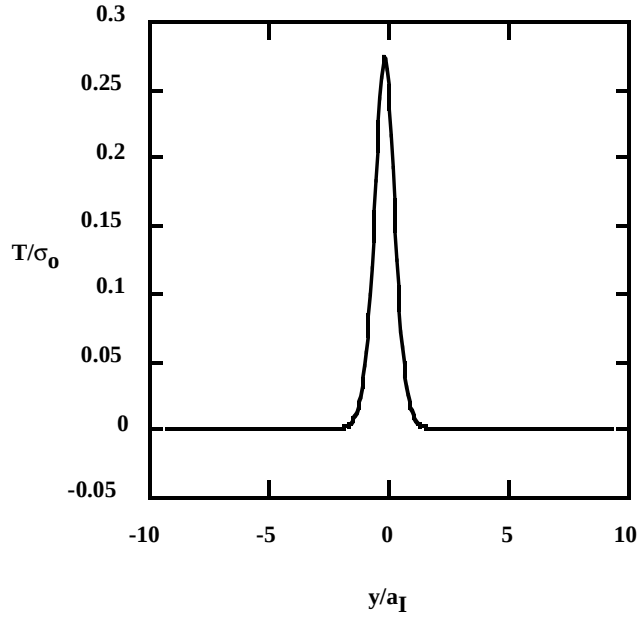

Fig. 6. The dimensionless difference, $T_A(y)/\sigma_0$, between the A-shear stress and A-monomer density profile, for the asymmetric blend of Figure 5.

dependence on R_g/a_I, equation (8.5) is a good approximation for the interfacial viscosity for $a_I/R_g \ll 1$. Thus the extrapolation length shows the same scaling with χ as the symmetric blend.

Next, consider the case where $w = 1$ and $R_{g,A} \neq R_{g,B}$. Notice that for the symmetric blend, the effect of R_g on the interfacial viscosity comes in through the parameter $(a_I/R_g)^2$ (see Eq. (6.10)), *i.e.* in the way that the interfacial viscosity heals back to the bulk viscosity. This parameter is small, but finite, in our numerical work[5], so errors on the order of $(a_I/R_g)^2$ are introduced. We expect that asymmetry in the R_g's should shift the position and magnitude of the peak in the shear rate, since the interfacial viscosity must heal back to two different bulk viscosities. Numerics (with w held fixed) show that varying the ratio $R_{g,A}/R_{g,B}$ has only a slight effect on the shear rate, which is on the same order as the finite-R_g errors.

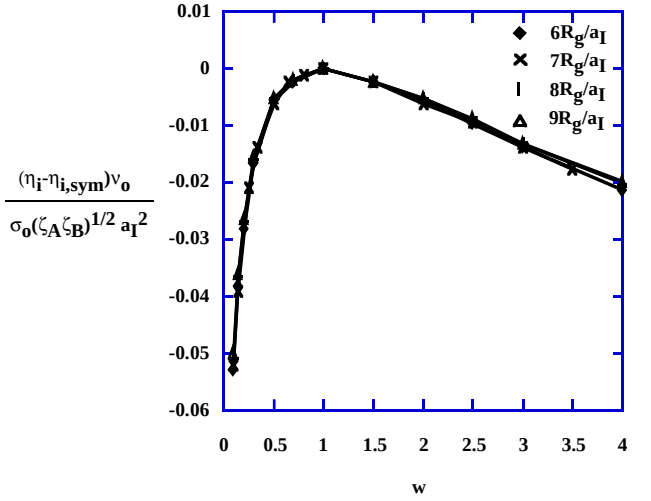

Fig. 7. Normalized interfacial viscosity as a function of the friction coefficient ratio, w, for fixed R_g/a_I, $\chi = 0.1, \zeta_A = 1$. Here, we show four different values of R_g/a_I for which equation (8.5) is a good approximation.

We have neglected the concentration dependence of the friction coefficients in this analysis, which a realistic treatment of an asymmetric blend should necessarily include. In addition, because of the difference in elasticity and viscosity between the two species, asymmetric blends can exhibit instabilities under shear [22] due to normal stress differences between the two phases. Certainly, instabilities due to viscosity and density differences are known for purely Newtonian phase-separated fluids. Consequently, a highly asymmetric blend might produce very different dynamics experimentally than those considered here. This is an interesting situation that we leave for future work.

9 Phenomenological extension to the entangled case

Let us now consider a symmetric entangled blend. There are two possible cases:
i) where the tube diameter of the entanglement network is

[5] There are numerical difficulties associated with using an integration range much larger than about $9a_I$, which in turn limits the chain radius of gyration. However, since gradients in shear rate and stress do not change significantly beyond a_I, this does not affect the position and magnitude of the maximum shear rate, or the shape of these curves. We have checked this by systematically varying the integration range.

larger than the interfacial width and Rouse friction dominates in the interface, and
ii) where the tube diameter is smaller than the interfacial width so that entanglement dynamics come into play in the interface.

We use an argument due to de Gennes [8] to distinguish between these two regimes. As we discussed in Section 2, the interface consists mostly of loops of length s, with average length $s^* \sim 1/\chi$. We write the probability distribution of loops as

$$p(s) = \frac{\exp\left[-\frac{\Delta H}{k_{\rm B}T}\right]}{s^*} \tag{9.1}$$

where $\Delta H = \chi s k_{\rm B}T$. Loops can effectively entangle only if they are longer than the distance between entanglements, $N_{\rm e}$ [7]. We may estimate the fraction of such loops, f as follows

$$f = \sum_{N_{\rm e}}^{\infty} p(s) \approx \exp[-N_{\rm e}\chi] \propto \exp\left[-\left(\frac{D}{a_{\rm I}}\right)^2\right] \tag{9.2}$$

where $D \propto N_{\rm e}^{1/2} b$ denotes the tube diameter. Thus Rouse dynamics dominate for $\chi N_{\rm e} \gg 1$ and entanglement dynamics for $\chi N_{\rm e} \ll 1$.

9.1 D ≫ a_I: Rouse-like interfacial friction

Here we can use an equation similar to equation (6.1), except that we must change the coefficient of the term linear in the stress to reflect the bulk viscosity of the entangled melt outside the interface.

$$0 = \kappa(y)\sigma_{yy} + \frac{1}{\zeta}U'\sigma'_{xy} - \frac{2}{\zeta {R_{\rm g}}^2 (N/N_{\rm e})^2}\sigma_{xy} - \frac{1}{\zeta}\frac{\phi'}{\phi}\sigma'_{xy} + \frac{1}{\zeta}\sigma''_{xy}. \tag{9.3}$$

This equation then produces Rouse-like dynamics in the interface, and we should use the Rouse concentration equation (4.5) in conjunction with it. Repeating the analysis of Section 6 we find that the extrapolation length in this case is

$$|l_{\rm e}| = \frac{\sqrt{6\chi} R_{\rm g}^2 (N/N_{\rm e})^2}{2b} \tag{9.4}$$

which is once more in agreement with the scaling prediction of reference [8]. For $\chi \approx 0.1, b \approx 3$ Å, $N \approx 10^3, N_{\rm e} \approx 10^2$, we get $l_{\rm e} \approx 10$ μm, which is considerably larger than that for the Rouse melt. (Since we are mainly concerned with investigating the Rouse dynamics in the interface, we do not attempt to reproduce the non-linear viscoelasticity of the outer entangled melt in Eq. (9.3). However, we shall address this point in the next section.)

9.2 D ≪ a_I: Reptation-like interfacial friction

We now consider a symmetric blend where the tube diameter is smaller than the interfacial width, so that the chains are long enough that entanglement effects become significant, both in the bulk and the interface. In Appendix B, we derive the concentration equation for an entangled melt, using a two-fluid scheme developed by Doi and Onuki [23] for Rouse solutions and asymmetric entangled melts.

$$\frac{\partial \phi}{\partial t} = -\boldsymbol{\nabla}\cdot(\phi \mathbf{v}) + \frac{1}{\zeta(N/N_{\rm e})}\boldsymbol{\nabla}\cdot[\phi\boldsymbol{\nabla}U - \nu_0 \boldsymbol{\nabla}\cdot\boldsymbol{\sigma}]\,. \tag{9.5}$$

Notice that this equation has exactly the same form as the concentration equation for the Rouse melt (Eq. (4.5)), except that the friction coefficient has been renormalized by $(N/N_{\rm e})$. (The noise term is absent but we shall remedy that shortly.)

We should point out that the stress $\boldsymbol{\sigma}$ in equation (9.5) has a different interpretation from the stress in the Rouse model. The reptation model [7] focuses on the primitive chain, for which only $N/N_{\rm e}$ segments are active in supporting stress. Consequently, the concentration associated with this reptation stress is the actual concentration divided by $N_{\rm e}$. In the absence of any external potential or flow fields, the reptation stress reduces to an isotropic tensor $\boldsymbol{\delta}\phi/\nu_0$, where ϕ is the renormalized concentration, *i.e.* the concentration of entanglement segments. The noise term is then simply $(1/\zeta(N/N_{\rm e}))\nabla^2\phi$, which is entirely analogous to that for the Rouse melt. The deviatoric stress is therefore defined as $\boldsymbol{\Sigma} = \boldsymbol{\sigma} - \boldsymbol{\delta}\phi/\nu_0$.

Since the form of the concentration equation is identical to that of the Rouse melt except that the coefficients are renormalized, we are led to write a stress constitutive equation having the same form as the Rouse model, but with different coefficients.

In order to obtain the bulk entanglement viscosity $\zeta N(N/N_{\rm e})^2/2$, the coefficient of the Σ term in equation (6.1) must be $2/\zeta N(N/N_{\rm e})^2$. Thus the terms involving gradients of the stress and the density ought also to gain a factor of $(N/N_{\rm e})^2$. The potential terms must be renormalized in the same way so that the analog of equation (4.6) is satisfied at equilibrium. The analog of equation (6.1) for the entangled melt is therefore

$$0 = \kappa(y)\sigma_{yy} + \frac{1}{\zeta\left(\frac{N}{N_{\rm e}}\right)^2}U'\sigma'_{xy} - \frac{2}{\zeta {R_{\rm g}}^2\left(\frac{N}{N_{\rm e}}\right)^2}\sigma_{xy} - \frac{1}{\zeta\left(\frac{N}{N_{\rm e}}\right)^2}\frac{\phi'}{\phi}\sigma'_{xy} + \frac{1}{\zeta\left(\frac{N}{N_{\rm e}}\right)^2}\sigma''_{xy}\,. \tag{9.6}$$

Using this model for an entangled symmetric blend, the characteristic scale of the interfacial viscosity is $\zeta b^2/(6\chi\nu_0(N/N_{\rm e})^2)$, which is the scale-dependent entanglement viscosity [8], analogous to the scale-dependent Rouse viscosity. The extrapolation length in this case is $|l_{\rm e}| = \sqrt{6\chi}R_{\rm g}^2/2b$ and differs from the Rouse extrapolation length only by a prefactor. Of course since our model

is purely phenomenological, all numerical prefactors are questionable. In addition, the existence of a characteristic scale for the interfacial viscosity can only be verified through a microscopic model. Since the entanglement-like interfacial viscosity is $(N/N_e)^2$ times larger than the Rouse-like interfacial viscosity, we see that the interfacial slip will be markedly different depending on the value of χN_e.

Note that that the reptation model, unlike the Rouse model, exhibits a non-zero second normal stress difference [7], so we expect the concentration and stress profiles to be shear rate dependent (which we did not find for the case of the Rouse model in Sect. 6).

For homogeneous entangled melts, Larson [22] has presented a simple constitutive equation (which is a good approximation to the Doi-Edwards constitutive equation [7]):

$$\frac{\mathrm{D}\boldsymbol{\sigma}}{\mathrm{D}t} - (\boldsymbol{\nabla}\mathbf{v})^{\mathrm{T}} \cdot \boldsymbol{\sigma} - \boldsymbol{\sigma} \cdot \boldsymbol{\nabla}\mathbf{v} + \frac{2}{3G_e}\mathbf{D} : \boldsymbol{\sigma}\boldsymbol{\sigma} + \frac{1}{\tau_d}(\boldsymbol{\sigma} - G_e\boldsymbol{\delta}) = 0 \quad (9.7)$$

where $G_e = \phi$ is the shear modulus, $\tau_d = N^3/N_e$ is the disengagement time [7], and $2\mathbf{D} = [\boldsymbol{\nabla}\mathbf{v} + (\boldsymbol{\nabla}\mathbf{v})^{\mathrm{T}}]$ is the symmetric rate of strain tensor. Notice that equation (9.7) differs from equation (6.12) only by the term $(2/3G_e)\mathbf{D} : \boldsymbol{\sigma}\boldsymbol{\sigma} = (2/3G_e)D_{lk}\sigma_{il}\sigma_{jk}$, which incorporates non-linear viscoelastic effects into the bulk melt.

We may similarly adapt the flow terms in our constitutive equation to reflect this non-linearity. We then have the following equation set for σ_{xy}, σ_{yy} and ϕ respectively, for the A-species:

$$0 = \kappa(y)\left[\sigma_{yy} + \frac{1}{3\phi}(\sigma_{xx}\sigma_{yy} + \sigma_{xy}^2)\right] + \frac{1}{\zeta(\frac{N}{N_e})^2}U'\sigma'_{xy} - \frac{2}{\zeta {R_g}^2(\frac{N}{N_e})^2}\sigma_{xy} - \frac{1}{\zeta(\frac{N}{N_e})^2}\frac{\phi'}{\phi}\sigma'_{xy} + \frac{1}{\zeta(\frac{N}{N_e})^2}\sigma''_{xy} \quad (9.8)$$

$$0 = \kappa(y)\left[\frac{2}{3\phi}\sigma_{xy}\sigma_{yy}\right] + \frac{1}{\zeta(\frac{N}{N_e})^2}[U'\sigma'_{yy} - U''\sigma_{yy}] - \frac{2}{\zeta R_g^2(\frac{N}{N_e})^2}\Sigma_{yy} - \frac{1}{\zeta(\frac{N}{N_e})^2}2\frac{\phi'}{\phi}\Sigma'_{yy} + \frac{1}{\zeta(\frac{N}{N_e})^2}\Sigma''_{yy} \quad (9.9)$$

$$0 = -(\phi U') + (\nu_0 {\sigma_{yy}}' - \phi') \quad (9.10)$$

which together with a similar set for the B-species must be solved under the shear stress and density constraints. An important difference from the Rouse equations of Section 6, is that the σ_{yy}-equation is now coupled to the shear stress and shear rate through the term arising from $\mathbf{D} : \boldsymbol{\sigma}\boldsymbol{\sigma}$. This equation set is non-trivial to solve even perturbatively, since substituting equation (9.10) into equation (9.9) results in an integro-differential equation.

However, we can ask at what flow strength this additional coupling becomes significant. From equation (9.9), this term is important for the bulk dynamics when $\kappa \sim \phi N^3/N_e$. We recall, however, that ϕ has been normalized by N_e, *i.e.* bulk non-linear effects become important for $\kappa\tau_d \sim 1$. In the interface, chain dynamics occur on smaller scales, so that $\kappa\tau_d \gg \chi N$ for the coupling term to come into play. (We have balanced the coupling term against the gradient terms in Eq. (9.9) to obtain this result). Since $\chi N \gg 1$ for a strongly-segregated blend, we see that a substantial flow strength is needed to cause deviations from the equilibrium interfacial width and concentration profile.

10 Conclusions

We have developed a constitutive equation for stress relaxation in a strongly inhomogeneous polymer melt obeying Rouse dynamics. This equation is then used to calculate the viscosity of a symmetric homopolymer blend. We find the viscosity in the interface is $\zeta b^2/(6\chi\nu_0)$ in agreement with the scaling prediction of reference [8]. This treatment can be extended phenomenologically to the entangled case to produce a crossover from Rouse friction in the interface to reptation dynamics in the bulk.

It should be possible to test our prediction for the shear rate by using tagged particles to visualize velocity profiles. A model system might be a blend of deuterated and undeuterated homopolymers, where the deuteration provides sufficient incompatibility to cause phase segregation, without changing the chain mobilities significantly.

A more accessible experimental quantity is the apparent viscosity of the blend. This is given by $\eta_{\mathrm{app}} = \eta_0/[1+2l_e/L]$, where L is the system size, and $l_e \sim a_I\eta_0/\eta_i$ denotes the extrapolation length (which characterizes the apparent "velocity jump" due to the presence of the interface). For bulk blends, L is generally larger than l_e, and so the apparent viscosity should be close to the bulk viscosity. In layered entangled systems with Rouse-like interfacial friction, however, the extrapolation length can be many times the layer size. Experiments [24] on coextruded laminates of two homopolymers, with a layer thickness of 50 μm, measured an apparent viscosity of $\eta_{\mathrm{app}} \sim \eta_0/20$. Here, η_0 was the bulk average viscosity of the two homopolymers, showing that interfacial slip can have remarkable effects on the flow properties of these structured systems.

Interfacial slip can also be significant in polymer emulsification. For Newtonian emulsions, increasing the viscosity of the inner fluid relative to that of the outer fluid can cause the drag on a deformable droplet to be that on a hard sphere [25]. For polymeric fluids, interfacial slip at the drop surface can reverse this effect when the extrapolation length is many times the droplet size. The addition of block copolymer to such interfaces subsequently changes the slip properties.

We have also extended our analysis to asymmetric blends. In the symmetric blend, inhomogeneity is introduced only through the effects of an external potential. For asymmetric blends, the difference in elasticity or viscosity between the two components can cause the interface to become unstable under shear. We have not explored this intriguing aspect of the problem.

We are grateful to L. Leibler for helpful discussions. This work was supported by the MRL program of the National Science Foundation under Award Number DMR96-32716.

Appendix A: Constructing the Green's function

We show here how to construct a Green's function for equation (6.5) using the method of matched asymptotic expansions. (The following derivation is for the A-species; we suppress the A-subscript for conciseness. The analysis for the B-species is entirely analogous).

The Green's function $G(a,y)$ is the solution to

$$-\frac{6}{R_g^2}T - \frac{\phi'}{\phi}T' + T'' = \delta(y-a). \tag{A.1}$$

In solving the homogeneous equation, we realize that there are two important regimes: an "inner" regime on the scale of the interface where the dominant terms of equation (A.1) are

$$-\frac{\phi'}{\phi}T' + T'' = 0 \tag{A.2}$$

with the solution

$$T_{\text{inner}} = C_1 \int_0^y \phi(x)\mathrm{d}x + C_2 \tag{A.3}$$

and an "outer" region for scales on the order of the chain radius of gyration. (In this regime the interface "appears" to be at $y = 0$.) Here equation (A.1) may be written approximately as

$$-\frac{6}{{R_g}^2}T + T'' = 0. \tag{A.4}$$

The outer solution is given by

$$T_{\text{outer}} = C_3 \exp\left[\frac{\sqrt{6}y}{R_g}\right] + C_4 \exp\left[\frac{-\sqrt{6}y}{R_g}\right]. \tag{A.5}$$

A uniform solution for T exists if the two solutions have a common limit in a "matching" regime where $a_I \ll y \ll R_g$. To identify this limit, we take the outer limit of the inner solution and the inner limit of the outer solution. For $y > 0$

$$y \to \infty, \quad T^+_{\text{inner}} \to C_1^+[\frac{a_I}{4}\ln\frac{1}{2} + y] + C_2^+$$
$$y \to 0, \quad T^+_{\text{outer}} \to [C_3^+ - C_4^+]\frac{\sqrt{6}}{R_g}y + [C_3^+ + C_4^+].$$

The solutions match if $C_1^+ = (C_3^+ - C_4^+)\sqrt{6}/R_g$ and $C_2^+ = C_3^+ + C_4^+ - C_1^+(a_I/4)\ln(1/2)$. The uniform solution is thus given by

$$T^+ = C_3^+\left[\exp\left(\frac{\sqrt{6}y}{R_g}\right) - \frac{\sqrt{6}}{R_g}\frac{a_I}{4}\ln\phi\right] + C_4^+\left[\exp\left(-\frac{\sqrt{6}y}{R_g}\right) + \frac{\sqrt{6}}{R_g}\frac{a_I}{4}\ln\phi\right]. \tag{A.6}$$

Similarly matching for $y < 0$

$$y \to -\infty, \quad T^-_{\text{inner}} \to C_1^-\mu + C_2^-$$
$$y \to 0, \quad T^-_{\text{outer}} \to [C_3^- - C_4^-]\frac{\sqrt{6}}{R_g}y + [C_3^- + C_4^-]$$

where $\mu = \int_0^{-\infty}\phi(x)\mathrm{d}x = -(a_I/4)\ln(1/2)$, and we identify $C_3^- + C_4^- = 0, C_1^-\Gamma + C_2^- = C_3^- + C_4^-$. The uniform solution for $y < 0$ is then

$$T^- = C_1^-\frac{a_I}{4}\ln[1-\phi] + C_3^-\left[\exp\left(\frac{\sqrt{6}y}{R_g}\right) + \exp\left(-\frac{\sqrt{6}y}{R_g}\right)\right]. \tag{A.7}$$

A solution for all y is written as

$$T = [Af_1(y) + Bf_2(y)]\theta(y) + [Cf_3(y) + Df_4(y)]\theta(-y) \tag{A.8}$$

where

$$\theta(y) = \begin{cases} 1 & y > 0 \\ 0 & y < 0 \end{cases}$$

$$f_1(y) = \exp\left(\frac{\sqrt{6}y}{R_g}\right) - \frac{\sqrt{6}}{R_g}\frac{a_I}{4}\ln\phi \tag{A.9}$$

$$f_2(y) = \exp\left(-\frac{\sqrt{6}y}{R_g}\right) + \frac{\sqrt{6}}{R_g}\frac{a_I}{4}\ln\phi \tag{A.10}$$

$$f_3(y) = \frac{a_I}{4}\ln[1-\phi] \tag{A.11}$$

$$f_4(y) = \exp\left(\frac{\sqrt{6}y}{R_g}\right) + \exp\left(-\frac{\sqrt{6}y}{R_g}\right). \tag{A.12}$$

To find the Green's function $G(a,y)$ we must consider three separate cases

i) $a > 0$

$$y < a \quad G(a,y) = A(a)f_1(y) + B(a)f_2(y)$$
$$y > a \quad G(a,y) = [A^*(a)f_2(y) + B^*(a)f_2(y)]\theta(y) + [C^*(a)f_3(y) + D^*(a)f_4(y)]\theta(-y). \tag{A.13}$$

The six constants are determined by requiring that

1) $G(a,y)$ is continuous at $y = a$,
2) $\partial G/\partial y$ has a finite jump discontinuity of magnitude unity at $y = a$,
3) $G(a,+\infty) = 0$,
4) $G(a,-\infty) = 0$,
5) $G(a,y)$ is continuous at $y = 0$ and
6) $\partial G/\partial y$ is continuous at $y = 0$.

ii) $a < 0$

Here we write

$$y < a \quad G(a,y) = [A(a)f_1(y) + B(a)f_2(y)]\theta(y) + [C(a)f_3(y) + D(a)f_4(y)]\theta(-y)$$
$$y > a \quad G(a,y) = C^*(a)f_3(y) + D^*(a)f_4(y). \tag{A.14}$$

The constants are determined using the same conditions as in (i).
iii) $a = 0$

$$\begin{aligned} y < a \quad & G(a,y) = \quad A(a)f_1(y) + B(a)f_2(y)] \\ y > a \quad & G(a,y) = \quad C^*(a)f_3(y) + D^*(a)f_4(y). \end{aligned} \tag{A.15}$$

In this case we only need to satisfy conditions (1)-(4) given in (i).

Appendix B: The concentration equation for an entangled melt

(In this section, we borrow heavily from Ref. [23] to where the reader is referred for details). Let $\mathbf{v}_{\rm A}(\mathbf{r},t)$ and $\mathbf{v}_{\rm B}(\mathbf{r},t)$ denote the velocities of A and B chains respectively, where the volume average velocity is given by

$$\mathbf{v} = \phi\mathbf{v}_{\rm A} + (1-\phi)\mathbf{v}_{\rm B}. \tag{B.1}$$

The conservation equation for the A-polymer mass density is

$$\frac{\partial\phi}{\partial t} = -\boldsymbol{\nabla}\ \cdot\ (\phi\mathbf{v}_{\rm A}) \tag{B.2}$$

and similarly for the B-species. To find $\mathbf{v}_{\rm A}$ and $\mathbf{v}_{\rm B}$, we shall use Rayleigh's variational principle, where the following "Rayleighian" function is to be minimized with respect to the two velocities

$$R = \frac{1}{2}W + \dot{F} \tag{B.3}$$

where W is the energy dissipation rate and is $\dot{F}$ is the free energy change in the system.

Each polymer species is assumed to move through a tube created by the entanglement network, which is itself moving at a velocity $v_{\rm T}$. The curvilinear velocity ω_i of a polymer along its own tube is related to its center of mass velocity as

$$v_i - v_{\rm T} = \frac{\omega_i h_i}{L_i} \tag{B.4}$$

where h_i and L_i denote the end-to-end distance and tube contour length of the i-species respectively. At equilibrium $(L_i/h_i)^2 = N_i/N_{{\rm e},i}$ where $N_{{\rm e},i}$ is the number of monomers between entanglement points. (We shall assume that this relation continues to hold under weak flow conditions).

The energy dissipation arises from the relative motion between the polymers and the entanglement network and is written as

$$W = \int \mathrm{d}\mathbf{r}[\phi_{\rm A}\zeta_{\rm A}\omega_{\rm A}^2 + \phi_{\rm B}\zeta_{\rm B}\omega_{\rm B}^2]. \tag{B.5}$$

The tube velocity $v_{\rm T}$ is determined by requiring that the frictional force on the network balance *i.e.* $(\frac{1}{2})\delta W/\delta v_{\rm T} = 0$. Using equations (B.4, B.5) we get

$$\phi_{\rm A}\frac{N_{\rm A}}{N_{\rm e,A}}\zeta_{\rm A}(v_{\rm A} - v_{\rm T}) + \phi_{\rm B}\frac{N_{\rm B}}{N_{\rm e,B}}\zeta_{\rm B}(v_{\rm B} - v_{\rm T}) = 0 \tag{B.6}$$

so that for a symmetric melt the tube velocity reduces to the volume average velocity.

Substituting equations (B.4, B.6) into equation (B.5), we obtain for a symmetric blend

$$W = \int \mathrm{d}\mathbf{r}\ \zeta\frac{N}{N_{\rm e}}\phi_{\rm A}\phi_{\rm B}(v_{\rm A} - v_{\rm B})^2. \tag{B.7}$$

There are two contributions to the free energy change. The first is due to the external potential (which we recall involves both the A-B contact energy and a potential to maintain melt incompressibility) written as

$$\begin{aligned} \dot{F}_{\rm m} &= \int \mathrm{d}\mathbf{r}\left[\frac{\delta F_{\rm m}}{\delta\phi_{\rm A}}\dot{\phi}_{\rm A} + \frac{\delta F_{\rm m}}{\delta\phi_{\rm B}}\dot{\phi}_{\rm B}\right] \\ &= -\int \mathrm{d}\mathbf{r}\left[\frac{\delta F_{\rm m}}{\delta\phi_{\rm A}}\boldsymbol{\nabla}\cdot(\phi_{\rm A}\mathbf{v}_{\rm A}) + \frac{\delta F_{\rm m}}{\delta\phi_{\rm B}}\boldsymbol{\nabla}\cdot(\phi_{\rm B}\mathbf{v}_{\rm B})\right] \end{aligned} \tag{B.8}$$

where $F_{\rm m} = \int \mathrm{d}\mathbf{r}[U_{\rm A}\phi_{\rm A} + U_{\rm B}\phi_{\rm B}]$. The second contribution arises from the change in the elastic energy of the polymers which we write as

$$\dot{F}_{\rm e} = \int \mathrm{d}\mathbf{r}[\boldsymbol{\sigma}_{\rm A} : \nabla\mathbf{v}_{\rm A} + \boldsymbol{\sigma}_{\rm B} : \nabla\mathbf{v}_{\rm B}]. \tag{B.9}$$

The Rayleighian for the entangled melt is thus given by

$$\begin{aligned} R = \int \mathrm{d}\mathbf{r}\ \Big[&\frac{1}{2}\zeta\frac{N}{N_{\rm e}}\phi_{\rm A}\phi_{\rm B}(v_{\rm A} - v_{\rm B})^2 - \frac{\delta F_{\rm m}}{\delta\phi_{\rm A}}\boldsymbol{\nabla}\cdot(\phi_{\rm A}\mathbf{v}_{\rm A}) \\ &+\boldsymbol{\sigma}_{\rm A}{:}\boldsymbol{\nabla}\mathbf{v}_{\rm A} + \boldsymbol{\sigma}_{\rm B}{:}\boldsymbol{\nabla}\mathbf{v}_{\rm B}]\,. \end{aligned} \tag{B.10}$$

From $\delta R/\delta v_{\rm A} = 0$, equations (B.1, B.2), we obtain the concentration equation for the A-species

$$\frac{\partial\phi_{\rm A}}{\partial t} = -\boldsymbol{\nabla}\cdot(\phi_{\rm A}\mathbf{v}) + \frac{1}{\zeta(N/N_{\rm e})}\boldsymbol{\nabla}\cdot[\phi_{\rm A}\boldsymbol{\nabla}U_{\rm A} - \boldsymbol{\nabla}\cdot\boldsymbol{\sigma}_{\rm A}]\,. \tag{B.11}$$

References

1. P.A. Drda, S.Q. Wang, Phys. Rev. Lett. **75**, 2698 (1995).
2. K.B. Migler, H. Hervet, L. Leger, Phys. Rev. Lett. **70**, 287 (1993).
3. D. Ausserre, J. Edwards, J. LeCourtier, H. Hervet, F. Rondelez, Europhys. Lett., **14**, 33 (1991).
4. L.A. Archer, R.G. Larson, Y.L. Chen, J. Fluid Mech. **301**, 133 (1995).
5. F. Brochard-Wyart, C. Gay, P.G. de Gennes, Macromolecules **29**, 377 (1996).
6. A. Ajdari, F. Brochard-Wyart, P.G. de Gennes, L. Leibler, J.L. Viovy, M. Rubinstein, Physica A **204**, 17 (1994).
7. M. Doi, S.F. Edwards, *The Theory of Polymer Dynamics* (Oxford University Press, Oxford 1986)
8. i) P.G. de Gennes, C.R. Acad. Sci. **308 II**, 1401 (1989); ii) F. Brochard, P.G. de Gennes, S. Troian, C.R. Acad. Sci. Paris **310 III**, 1169 (1990); iii) de Gennes, P.G. *Physics of Polymer Surfaces and Interfaces*, edited by Isaac C. Sanchez (Butterworth-Heinemann, Massachusetts, 1992), Chap. 3, p. 55.

9. G.H. Fredrickson, F.S. Bates, Ann. Rev. Mater. Sci. **26**, 501 (1996).
10. E. Helfand, G.H. Fredrickson, Phys. Rev. Lett. **62**, 2468 (1989).
11. i) S.T. Milner, Phys. Rev. Lett. **66**, 1477 (1991); ii) Phys. Rev. E. **48**, 3674 (1992).
12. C.F. Curtiss, R.B. Bird, Adv. Polym. Sci **125**, 1 (1996).
13. H.C. Ottinger, J. Chem. Phys. **84**, 4068 (1986).
14. V.G. Mavrantas, A.N. Beris, Phys. Rev. Lett. **69**, 273 (1992).
15. A.W. El-Kareh, L.G. Leal, J. Non-Newtonian Fluid Mechanics **33**, 257 (1989).
16. A.V. Bhave, R.C. Armstrong, R.A. Brown, J. Chem. Phys. **95**, 2988 (1991).
17. E. Helfand, Y. Tagami, J. Chem. Phys. **56**, 3592 (1971).
18. P.G. de Gennes, *Scaling Concepts in Polymer Physics* (Cornell University Press, Ithaca 1979), Chap. 9, p. 250.
19. K. Kawasaki, K. Sekimoto, Physica (Amsterdam) **143A**, 349 (1987).
20. A.N. Beris, V.G. Mavrantas, J. Rheol. **38**, 1235 (1994).
21. R.G. Larson, *Constitutive Equations for Polymer Melts and Solutions* (Butterworth, Boston 1988), Chap. 1, p. 25.
22. R.G. Larson, Rheol. Acta **31**, 213 (1992).
23. M. Doi, A. Onuki, J. Phys. II France **2**, 1631 (1992).
24. A. Miroshnikov, Vysokomol Soedin. Ser. A (USSR) **29**, 579 (1987).
25. L.G. Leal, *Laminar Flow and Convective Transport Processes* (Butterworth-Heinemann, 1992), p. 251.